INSTITUTE FOR FUSION STUDIES

DE-FG05-80ET-53088-713 IFSR #713

Simulation of Alfvén Wave-Resonant Particle Interaction

H.L. BERK, B.N. BREIZMAN, and M. PEKKER
Institute for Fusion Studies
The University of Texas at Austin
Austin, Texas 78712 USA

July 1995

THE UNIVERSITY OF TEXAS

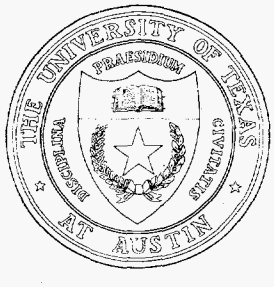

AUSTIN

DISCLAIMER

Portions of this document may be illegible in electronic image products. Images are produced from the best available original document.

Simulation of Alfvén wave-resonant particle interaction

H.L. Berk, B.N. Breizman, and M. Pekker
Institute for Fusion Studies, The University of Texas at Austin
Austin, Texas 78712 USA

Abstract

New numerical simulations are presented on the self-consistent dynamics of energetic particles and a set of unstable discrete shear Alfvén modes in a tokamak. Our code developed for these simulations has been previously tested in the simulations of the bump-on-tail instability model. The code has a Hamiltonian structure for the mode-particle coupling, with the superimposed wave damping, particle source and classical relaxation processes. In the alpha particle-Alfvén wave problem, we observe a transition from a single mode saturation to the mode overlap and global quasilinear diffusion, which is qualitatively similar to that observed in the bump-on-tail model. We demonstrate a considerable enhancement in the wave energy due to the resonance overlap. We also demonstrate the effect of global diffusion on the energetic particle losses.

I. INTRODUCTION

There is now considerable number of investigations devoted to the study of the nonlinear consequences arising from the possible instability in a fusion producing experiment of the alpha particle products interacting with Alfvén waves. The particular mode of concern is the Toroidal Alfvén Eigenmode (TAE)[1,2] that can be destabilized by the universal instability drive[3] of the energetic particle's phase space gradient. Several experiments have observed this instability with energetic neutral beams[4,5] or with ion cyclotron frequency heating of plasmas[6,7]; and several particle simulation calculations have been made describing the saturation of this instability.[8–12]

In this work we present recent results of an approach described in Refs. 8 and 12 for the simpler two-stream instability problem. In past works[8,13] it has been noted that the alpha particle-Alfvén wave interaction can be described from the general point of view of weak turbulence. One starts from the equilibrium distribution function that is established from the balance of a source and a classical transport mechanism (in the present work the transport mechanism is modelled by particle annihilation). The equilibrium distribution that is established has "free energy" to cause instability of a discrete spectrum of waves when the contribution to the linear growth rate from the hot particles exceeds the damping rate of the wave in absence of the hot particle drive. If it is appropriate to assume that the particle-wave resonance interaction can be described without mode overlap occurring, the modes will saturate at an amplitude determined by the condition that the bounce frequency, ω_b, of a resonant particle trapped in the fields of the wave (ω_b is proportional to the square root of the field amplitude) is comparable to the linear growth rate. This scaling is evident from analytic analysis[14] and has been demonstrated in several simulations.[8–12] When resonance mode overlap occurs, there is an amplification of the release of the particle free energy to

wave energy,[8,12,13] which then gives rise to global particle transport. A modelling of this effect using quasilinear equations has been shown in the proceedings of this conference.[15] More quantitative understanding of the details of this transition and the consequences for the global transport of alpha particles, will certainly be the focus of future work.

In this paper we indicate how the Alfvén-energetic particle interaction can be cast in a standard form that has the same structure for resonant particles in any physical system. The simplest system is the one-dimensional bump-on-tail instability, for which results are given in Refs. 8 and 12. We start from the general Lagrangian form that describes particles and electromagnetic fields. To leading order, the bulk plasma motion depends only on the mode amplitudes of the linear waves of the system. Hence, using the results of linear theory, a wave Lagrangian can be formed for the combined response of the background plasma and the electromagnetic field, that depends only on the linear waves' amplitudes and phases. We then outline how the Lagrangian for the hot particles and their interaction with the linear waves can be reduced to a standard form.

Finally, we present our simulation results, where we choose a set of typical TAE waves. These simulations will show the transition of saturation from the case when multiple waves are present but the resonances do not overlap, to the case when the resonances overlap and may produce global particle transport.

The rest of the paper is organized as follows:

In Sec. II we derive a reduced Lagrangian for the nonlinear interaction of shear Alfvén waves with energetic particles that resonate with the waves. We will assume that the number of energetic particles is relatively small, so that these particles have no effect on the spatial structure of the waves. It is also essential that wave amplitudes remain small, so that the finite amplitude waves retain the structure of the linear eigenmodes which we assume to be Toroidicity-induced Alfvén Eigenmodes. The appropriate dynamical variables for these

waves are their amplitudes and phases, which change as the waves interact with resonant particles. In Sec. III, we present our numerical results on the simulation of: the dynamics of single mode saturation, resonance overlap between two neighboring modes, and the collective bursts with particle losses, respectively. Section IV contains a brief summary.

II. LAGRANGIAN FORMALISM FOR WAVE-PARTICLE INTERACTION

In this section we present the derivation of the simplified Lagrangian for energetic particles interacting with shear Alfvén waves in a cold plasma (zero beta limit).

Our starting point will be the exact Lagrangian for charged particles in an electromagnetic field

$$L = \sum_{\substack{\text{plasma}\\ \text{particles}}} \left[\frac{mv^2}{2} + \frac{e}{c}(\mathbf{A}\cdot\mathbf{v}) - e\phi\right] + \frac{1}{8\pi}\int (E^2 - B^2)dV$$

$$+ \sum_{\substack{\text{energetic}\\ \text{particles}}} \left[\frac{mv^2}{2} + \frac{e}{c}(\mathbf{A}\cdot\mathbf{v}) - e\phi\right]. \tag{1}$$

Since plasma particles have an adiabatic response to the fields, their contribution to the Lagrangian can be rewritten in terms of the field variables. With this simplification, the first two terms in Eq. (1) give a Lagrangian for the waves L_w:

$$L_w = \sum_{\substack{\text{plasma}\\ \text{particles}}} \left[\frac{mv^2}{2} + \frac{e}{c}(\mathbf{A}\cdot\mathbf{v}) - e\phi\right] + \frac{1}{8\pi}\int (E^2 - B^2)dV$$

$$- \sum_{\substack{\text{plasma}\\ \text{particles}}} \left[\frac{mv_0^2}{2} + \frac{e}{c}(\mathbf{A}_0\cdot\mathbf{v}_0) - e\phi_0\right] + \frac{1}{8\pi}\int (E_0^2 - B_0^2)dV \tag{2}$$

where subscripts "0" refers to the unperturbed quantities, and we have subtracted out a constant in the Lagrangian so that $L_w = 0$ when perturbations vanish.

It should be noted that, to lowest order, the wave Lagrangian L_w is quadratic with respect to the wave amplitudes since the linear terms vanish due to the fact that the equilibrium

state satisfies a minimum action principle.

Further manipulation is somewhat detailed and is left for a later paper to exhibit. One finds that to quadratic order in the fields, in a zero beta system, and in a gauge where the perturbed potential is zero, L_w can be reduced to:

$$L_w = \int d^3r \left\{ \frac{1}{8\pi v_A^2} \dot{\mathbf{A}}_{1\perp}^2 + \frac{J_\parallel}{2cB_0} \left(\mathbf{A}_{1\perp} \cdot \boldsymbol{\nabla} \times \mathbf{A}_{1\perp}\right) - \frac{(\nabla \times \mathbf{A}_{1\perp})^2}{8\pi} \right\} \tag{3}$$

where $\mathbf{A}_1$ is the perturbed vector potential, v_A is the Alfvén velocity, $J_\parallel$ is the unperturbed parallel plasma current. The dynamical variable in this Lagrangian is

$$\mathbf{A}_{1\perp} \equiv \mathbf{A}_1 - \frac{\mathbf{B}_0}{B_0} \left(\mathbf{A}_1 \cdot \mathbf{B}_0\right)$$

which we choose to represent by two independent scalar functions Φ and Ψ as follows:

$$\mathbf{A}_{1\perp} = \nabla\Phi - \mathbf{B}_0(\mathbf{B}_0 \cdot \nabla\Phi)/B_0^2 + \mathbf{B}_0 \times \boldsymbol{\nabla}\Psi/B_0. \tag{4}$$

One can show that if parallel gradients (along the magnetic field) are much less than the perpendicular gradients, a Ψ excitation which gives rise to magnetic compression is nearly decoupled from a Φ excitation that gives rise to magnetic shear. Hence, for the shear Alfvén-like excitation, we need only Φ. This then yields the following term for the reduced Lagrangian.

$$L_w = \frac{1}{8\pi} \int \left\{ \frac{1}{v_A^2} (\boldsymbol{\nabla}_\perp \dot{\Phi})^2 - \left[B_0 \boldsymbol{\nabla}_\perp \frac{1}{B_0^2} \left(\mathbf{B}_0 \cdot \boldsymbol{\nabla}\Phi\right) \right]^2 \right.$$

$$\left. - (\text{curl } \mathbf{B}_0)^2 \left[\frac{1}{B_0^2} \left(\mathbf{B}_0 \cdot \boldsymbol{\nabla}\Phi\right) \right]^2 - \frac{1}{B_0^2} \left(\mathbf{B}_0 \cdot \boldsymbol{\nabla}\Phi\right)(\boldsymbol{\nabla}\Phi \cdot \Delta\mathbf{B}_0) \right\} dV. \tag{5}$$

By minimizing the action

$$S_w = \int L_w dt$$

with respect to Φ, we obtain the following linear eigenmode equation, which determines a set of eigenfrequencies $-\omega$ and eigenfunctions $\Phi_\omega(\mathbf{r})$:

$$\omega^2 \,\mathrm{div}\, \frac{1}{v_A^2} \nabla_\perp \Phi_\omega + (\mathbf{B}_0 \cdot \nabla) \left[\frac{1}{B_0^2} \,\mathrm{div}\, B_0^2 \nabla_\perp \frac{1}{B_0^2} (\mathbf{B}_0 \cdot \nabla \Phi_\omega) \right]$$

$$-(\mathbf{B}_0 \cdot \nabla) \left[\frac{(\mathrm{curl}\, \mathbf{B}_0)^2}{B_0^2} (\mathbf{B}_0 \cdot \nabla) \Phi_\omega \right] - \tfrac{1}{2} (\mathbf{B}_0 \cdot \nabla) \left[\frac{1}{B_0^2} (\nabla \Phi_\omega \cdot \Delta \mathbf{B}_0) \right]$$

$$- \tfrac{1}{2} (\Delta \mathbf{B}_0 \cdot \nabla) \left[\frac{1}{B_0^2} (\mathbf{B}_0 \cdot \nabla \Phi_\omega) \right] = 0. \tag{6}$$

In a tokamak, an eigenfunction can be written as

$$\Phi_\omega(\mathbf{r}) = e^{in\varphi} \sum_m \Phi_{n;m}(\psi) e^{-im\theta} \tag{7}$$

where n is a toroidal mode number, φ is the geometrical toroidal angle, θ is the poloidal angular coordinate, and ψ is a label of the flux surfaces.

We then represent Φ as a superposition of linear modes

$$\Phi = \sum_{\text{eigenmodes}} A(t) \Phi_\omega(\mathbf{r}) \exp(-i\alpha(t) - i\omega t) + \text{c.c.} \tag{8}$$

where mode amplitudes $A(t)$ and phases $\alpha(t)$ are slowly varying functions of time. This representation reduces L_w to

$$L_w = \sum_{\text{eigenmodes}} \frac{\dot{\alpha} A^2 \omega}{2\pi} \int \frac{|\nabla_\perp \Phi_\omega|^2}{v_A^2} \, dV. \tag{9}$$

In this expression, rapidly oscillating terms have been neglected. The eigenfunction Φ_ω can always be normalized by the condition

$$\frac{\omega}{2\pi} \int \frac{|\nabla_\perp \Phi_\omega|^2}{v_A^2} \, dV = 1, \tag{10}$$

so that L_w takes the form

$$L_w = \sum_{\text{eigenmodes}} \dot{\alpha} A^2. \tag{11}$$

In terms of A and α, the equations of motion for free waves become

$$\begin{aligned} \dot{A} &= 0 \\ \dot{\alpha} &= 0. \end{aligned} \tag{12}$$

It should be noted that Eqs. (9) and (11) exhibit a *universal* structure of the Lagrangian for the waves with slowly varying amplitude and phase, which is valid for weakly nonlinear systems. Note that the Lagrangian is proportional to $\dot{\alpha}A^2$. Specific features of the mode enter the Lagrangian only as a form factor.

We now consider the Lagrangian for energetic particle guiding center motion. One can show, starting from Littlejohn's Lagrangian,[16] that zeroth order Lagrangian that gives the equilibrium orbits, can be written in the form,[17]

$$L_{\text{part}} = P_\theta \dot{\theta} + P_\varphi \dot{\varphi} + \frac{mc}{e}\mu\dot{\xi} - H(P_\varphi; P_\theta; \theta; \mu) \tag{13}$$

where the canonical momenta, P_θ and P_φ are taken as dynamical variables. They are defined as:

$$P_\theta = \frac{eA_\theta}{c} + mv_\parallel \frac{B_\theta}{B_0} \tag{14}$$

$$P_\varphi = \frac{eA_\varphi}{c} + mv_\parallel \frac{B_\phi}{B_0} \tag{15}$$

where the φ and θ subscripts refer to covariant vector components of a vector, e.g. for a vector $\mathbf{F}$ we have

$$F_\varphi = \frac{\mathbf{F}\cdot\boldsymbol{\nabla}\theta\times\nabla\psi}{\boldsymbol{\nabla}\varphi\cdot\nabla\theta\times\boldsymbol{\nabla}\psi}, \qquad F_\theta = \frac{\mathbf{F}\cdot\boldsymbol{\nabla}\psi\times\boldsymbol{\nabla}\varphi}{\nabla\varphi\cdot\nabla\theta\times\boldsymbol{\nabla}\psi}.$$

The Hamiltonian H is defined as

$$H \equiv \mu B_0 + \frac{\left(P_\varphi - \frac{e}{c}A_\varphi\right)^2}{2m}\left(\frac{B_0}{B_\varphi}\right)^2. \tag{16}$$

The unperturbed motion conserves μ, P_φ, and the energy H. With these three conservation laws the motion is fully integrable, which allows a canonical transformation from the

variables $(P_\theta; P_\varphi; \mu; \theta; \varphi; \zeta)$ to the action-angle variables $\left(\tilde{P}_\theta; \tilde{P}_\varphi; \tilde{\mu}; \tilde{\theta}; \tilde{\varphi}; \tilde{\zeta}\right)$. The generating function $G_0\left[\tilde{P}_\theta; \tilde{P}_\varphi; \tilde{\mu}; \theta; \varphi; \zeta\right]$ of this transformation has the form

$$G_0 = \varphi \tilde{P}_\varphi + \zeta \frac{mc}{e} \tilde{\mu} + \int_0^\theta d\theta \, P_\theta \left[\widetilde{H}; \tilde{P}_\varphi; \tilde{\mu}; \theta\right] \tag{17}$$

where P_θ is the poloidal momentum at the particle orbit as a function of the old poloidal angle θ, the new momentum $\tilde{P}_\varphi$, and the energy $\widetilde{H}(\tilde{P}_\varphi; \tilde{P}_\theta)$. The function P_θ is implicitly given by the equation

$$H(\tilde{P}_\varphi; P_\theta; \theta; \tilde{\mu}) = \widetilde{H}.$$

In terms of the function G_0, the transformation is determined by the following equations

$$\begin{aligned} \tilde{\varphi} &= \frac{\partial G_0}{\partial \tilde{P}_\varphi}; \qquad & P_\varphi &= \frac{\partial G_0}{\partial \varphi} \\ \tilde{\theta} &= \frac{\partial G_0}{\partial \tilde{P}_\theta}; \qquad & \mu &= \frac{e}{mc} \frac{\partial G_0}{\partial \zeta} \\ \tilde{\zeta} &= \frac{e}{mc} \frac{\partial G_0}{\partial \tilde{\mu}}; \quad & P_\theta &= \frac{\partial G_0}{\partial \theta}. \end{aligned} \tag{18}$$

Once this transformation is performed, the Hamiltonian becomes independent of $\tilde{\theta}$ and $\tilde{\varphi}$, i.e. Eq. (13) takes the form

$$L_0 = \tilde{P}\dot{\tilde{\theta}} + \tilde{P}_\varphi \dot{\tilde{\varphi}} + \frac{mc}{e} \tilde{\mu} \dot{\tilde{\zeta}} - \widetilde{H}(\tilde{P}_\theta; \tilde{P}_\varphi; \tilde{\mu}). \tag{19}$$

It follows from Eq. (19) that, in the unperturbed motion $\tilde{P}_\theta$, $\tilde{P}_\varphi$, and $\tilde{\mu}$ are constant and also that $\tilde{\theta}, \tilde{\varphi}$, and $\tilde{\zeta}$ are linear functions of time:

$$\dot{\tilde{\theta}} \equiv \omega_{\tilde{\theta}} = \frac{\partial \widetilde{H}}{\partial \tilde{P}_\theta}; \quad \dot{\tilde{\varphi}} \equiv \omega_{\tilde{\varphi}} = \frac{\partial H}{\partial \tilde{P}_\varphi}; \quad \dot{\tilde{\zeta}} \equiv \omega_{\tilde{\zeta}} = \frac{e}{mc} \frac{\partial H}{\partial \tilde{\mu}}. \tag{20}$$

The quantities $\omega_{\tilde{\theta}}$, $\omega_{\tilde{\varphi}}$, and $\omega_{\tilde{\zeta}}$ are the unperturbed frequencies of the poloidal-, toroidal-, and gyro-motion, respectively.

To first order, the perturbed particle Lagrangian is dominantly given by

$$L_{\text{int}} = \frac{e}{c} \mathbf{A}_1 \cdot \dot{\mathbf{X}}$$

with $\mathbf{A}_1$ the perturbed vector potential and $\mathbf{X}$ the particle guiding-center coordinate. Using $\mathbf{A}_1 = \boldsymbol{\nabla}\Phi - \mathbf{B}_0(\mathbf{B}_0 \cdot \nabla\Phi)/B_0^2$, we find that to within a total derivative (which does not alter the Euler equations derived from the Lagrangian) the perturbed Lagrangian is given by

$$L_{\rm int} = -\frac{e}{c}\left[\frac{\partial\Phi}{\partial t} + v_\parallel(\mathbf{B}_0 \cdot \nabla\Phi)/B_0^2\right]$$

where $v_\parallel = [2(H - \mu B_0/2m]^{1/2}$. Then using Eqs. (118) and (119) we obtain

$$L_{\rm int} = \frac{e}{c}\sum_{\text{eigenmodes}} A(t)e^{-i\alpha - i\omega t}$$

$$\cdot \sum_m \Phi_{n;m}(\psi)e^{in\varphi - im\theta}\, i\left[\omega - v_\parallel \frac{\mathbf{B}_0}{B_0}\,(n\boldsymbol{\nabla}\varphi - m\boldsymbol{\nabla}\theta)\right] + \text{c.c.} \tag{21}$$

In this expression small higher order terms proportional to $\dot{A}$ and $\dot{\alpha}$ have been neglected.

Next, we change particle coordinates from ψ, θ, φ, and $v_\parallel$ to the action-angle variables. Taking into account that $L_{\rm int}$ is a periodic function of $\tilde{\varphi}$ and $\tilde{\theta}$, we rewrite Eq. (21) as a Fourier series in $\tilde{\theta}$, i.e.

$$L_{\rm int} = \sum_{\text{eigenmodes}} Ae^{-i\alpha - i\omega t}\, e^{in\tilde{\varphi}} \cdot \sum_\ell V_{\ell,n}(\tilde{P}_\varphi; \tilde{P}_\theta)e^{i\ell\tilde{\theta}} + \text{c.c.} \tag{22}$$

with the matrix element $V_{\ell;n}$ given by the equation

$$V_{\ell;n}(\tilde{P}_\varphi; \tilde{P}_\theta) = \frac{1}{(2\pi)}\int_0^{2\pi} d\tilde{\theta} \cdot e^{-i\ell\tilde{\theta} - in\tilde{\varphi}} \sum_m i\,\frac{e}{c}\left[\omega - v_\parallel \frac{\mathbf{B}_0}{B_0}\,(n\boldsymbol{\nabla}\varphi - m\boldsymbol{\nabla}\theta)\right]$$

$$\cdot\ e^{in\varphi - im\theta}\,\Phi_{n;m}(\psi). \tag{23}$$

Finally, we combine Eqs. (11), (19), and (22) into the total Lagrangian for particles and waves:

$$L = \sum_{\text{particles}} \tilde{P}_\varphi\dot{\tilde{\varphi}} + \tilde{P}_\theta\dot{\tilde{\theta}} + \frac{mc}{e}\tilde{\mu}\dot{\tilde{\zeta}} - H(\tilde{P}_\varphi; \tilde{P}_\theta; \tilde{\mu}) + \sum_{\text{eigenmodes}} \dot{\alpha}A^2$$

$$2\,\text{Re}\sum_{\substack{\text{particles,}\\ \text{eigenmodes}}} Ae^{-i\alpha - i\omega t + in\tilde{\varphi}} \sum_\ell V_{\ell,n}(\tilde{P}_\varphi; \tilde{P}_\theta)e^{i\ell\tilde{\theta}}. \tag{24}$$

III. SIMULATION TECHNIQUE AND NUMERICAL RESULTS

Our numerical algorithm is based on the map equations for particles and waves, which can be derived from the Lagrangian (24) by integrating the Euler equations over a finite time step that is small compared to the instability growth time but large compared to the typical wave period. This algorithm is a straightforward generalization of the algorithm developed in Ref. 12 for the one-dimensional bump-on-tail proble. In order to calculate the matrix element (23) we use an analytic approximation for the mode structure, which combines the asymptotic results of Refs. 18 and 19 and which is quantitatively valid in the low shear limit. Namely, we put

$$\Phi_\omega(\mathbf{r}) = \left(\frac{v_A \hat{\varepsilon} q(r_0)}{8\pi m_0}\right)^{1/2} e^{in\zeta - im_0\bar{\theta}} \left(1 + e^{-i\bar{\theta}}\right)$$
$$\cdot\ K_0\left(\frac{m_0}{r_0}\sqrt{(r-r_0)^2 + \left(\frac{r_0}{m_0}\hat{\varepsilon}\frac{\pi}{8}\right)^2}\right), \tag{25}$$

where $r, \zeta; \bar{\theta}$ are the straight field line coordinates, $K_0(x)$ is the zeroth-order Macdonald function, $\hat{\varepsilon} \equiv \frac{5}{2}\frac{r_0}{R}$, and r_0 is the gap location defined by the condition

$$q(r_0) = \frac{m_0 + 1/2}{n}.$$

We add to the wave evolution equation a damping rate due to the background plasma. The weights of the particles, w, are determined by the equation

$$\frac{dw}{dt} = -\nu_a w + S(\tilde{P}_\varphi, \tilde{P}_\theta)$$

where $S(\tilde{P}_\varphi, \tilde{P}_\theta)$ is a source for the particles (we take $\mu = 0$ in this simulation, a model for parallel beam injection in a tokamak), and ν_a is the annihilation rate. The validity of this procedure depends on the fact that the test particles move in an incompressible phase space. A formal demonstration of this statement is given in Ref. 12. The source is prepared to be spread about resonance curves in the $\tilde{P}_\theta, \tilde{P}_\varphi$ space. We denote the locus of points $(P_{\theta_0}, P_{\varphi_0})$

to be the curve that satisfies

$$\omega - n\bar{\omega}_\varphi(P_{\theta_0}, P_{\varphi_0}) - \ell\bar{\omega}_\theta(P_{\theta_0}, P_{\ell_0}) = 0.$$

This curve is indicated schematically in Fig. 1, by the broad solid line. Particles need to be loaded so that they encompass the region associated with the physical mode width plus the wings associated with finite orbit width. In addition there is the width due to the response of the particle to the wave. Near a single resonance curve, the resonance condition will be broadened by the trapping frequency $\omega_b \propto A^{1/2}$, of the particle in the wave, such that $\omega_b \approx \alpha\gamma_L$, where γ_L is the growth rate, α is a dimensionless number or order unity, and A the mode amplitude. This width, indicated in Fig. 1, has to be less than the particle loading width. The shaded area, in Fig. 1, indicates the window for particle loading. When more than one resonance is present, this loading needs to be implemented about each resonance. If global diffusion is to be described, the window around each resonance has to overlap the neighboring resonances.

The first type of simulation that is to be studied is the saturation of a single mode without sources and sinks. The linear growth rate is given by

$$\gamma_L = \pi \sum_{\substack{\text{particles,} \\ \text{sidebands } \ell}} |V_{\ell,n}|^2 \delta(\omega - n\bar{\omega}_\varphi - \ell\bar{\omega}_\theta) \cdot \left(n\frac{\partial F}{\partial \tilde{P}_\varphi} + \ell\frac{\partial F}{\partial \tilde{P}_\theta} \right)$$

where $V_{\ell,n}$ is the matrix element defined in Eq. (23) and F is the unperturbed distribution function of the energetic particles.

In Fig. 2 we show the saturation level $\alpha \equiv \omega_b/\gamma_L$ that arises when an unstable equilibrium distribution is initially loaded, and when there are no source, sink, or background damping. At sufficiently small γ_L/ω we see that $\alpha = 3.6$. There is a slight increase of α as γ_L/ω increases. This is probably due to a nonlinear effect that arises when a particle's displacement due to a finite wave becomes comparable to the orbit width.

In Fig. 3 we show the time evolution of a single mode when there is no mode overlap.

The parameters defining the mode are given in the figure caption. We see that the mode periodically bursts in time with an average wave energy release of less than 200 units.

In Fig. 4 we show the flattening of the distribution function as a function of radius. For this curve we have integrated the contribution over different particle velocities at the same radius. When two modes are loaded so that mode overlap can arise, we see in Fig. 5 that the wave energy release of a single mode with overlap is four times larger than in the no-overlap case (the second mode's characteristics are similar to the illustrated response), with longer intervals between bursts. The longer time is needed to reconstitute a distribution function that will produce a drive large enough to again cause overlap.

One can have many modes, without overlap, as seen in Fig. 6. We observe "benign" pulsations, without loss to a "particle collector plate" placed near the boundary of the system. However, when the growth rate is increased by 25%, it is enough to cause resonance overlap. We see in Fig. 7 that the overlapped modes cause a spatial flattening of the distribution function over all three modes. The wave energy release is enhanced by a factor of 50 compared to the non-overlapped case as seen in Fig. 8. The quivering of the orbits in these large amplitude waves brings the particles to the collector plates where they are absorbed.

IV. CONCLUSIONS

In this work we have indicated how a mapping method can be developed to describe TAE modes in a toroidal plasma. The mapping method has reduced the particle and wave equations to a universal form. By understanding the structure of resonance and transport between resonances a global picture of the nonlinear evolution can be inferred. This description applies equally well to the bump-on-tail instability described in earlier work, and to the simulation of TAE modes in a tokamak that have been described here.

Of course before one makes more quantitative comparisons with experiment, additional

work is needed to describe the wave mode structure and the resonance conditions in a realistic tokamak. Nonetheless, this work suggests that the particle loss observed in experiment[4,5] can be explained as due to the simultaneous onset of stochasticity with the amplification of wave energy. Both experiments show a rich spectral content of excited waves when particle losses are observed.

Acknowledgments

This work was supported by the U.S. Dept. of Energy contract No. DE-FG05-80ET-53088.

References

1. C.Z. Cheng, Liu Chen, and M.S. Chance, Ann. Phys. **161**, 21 (1985).

2. C.Z. Cheng and M.S. Chance, Phys. Fluids **29**, 3695 (1986).

3. L.I. Rudakov and R.Z. Sagdeev, Dokl. Akad. Nauk SSSR **138**, 58 (1961).

4. K.L. Wong, R.J. Fonck, S.F. Paul, D.R. Roberts, E.D. Fredrickson, R. Nazikian, H.K. Park, H. Bell, N.L. Bretz, R. Budny, S. Cohen, G.W. Hammett, F.C. Jobes, D.M. Meade, S.S. Medley, D. Mueller, Y. Nagayama, D.K. Owens, and E.J. Synakowski, Phys. Rev. Lett. **66**, 1874 (1991).

5. W.W. Heidbrink, E.J. Strait, E. Doyle, G. Sager, and R. Snider, Nucl. Fusion **31**, 1635 (1991).

6. K.L. Wong, J.R. Wilson, Z.Y. Chang, G.Y. Fu, E. Fredrickson, G.W. Hammet, C. Bush, C.K. Phillips, J. Snipest, and G. Taylor, Plasma Phys. Contrl. Fusion **36**, 879 (1994).

7. S. Ali-Arshad and D.J. Campbell, Preprint JET-DN-E(93) 33, 1993.

8. H.L. Berk, B.N. Breizman, and M. Pekker, in *Physics of High Energy Particles in Toroidal Systems*, AIP Conf. Proc. 311, edited by T. Tajima and M. Okamoto (American Institute of Physics, New York (1994) p. 18.

9. G.Y. Fu and W. Park, Phys. Rev. Lett. **74**, 1594 (1995).

10. Y. Todo, T. Sato, K. Watanabe, T.H. Watanabi, and R. Horiuchi, to be published in Phys. Plasmas.

11. Y. Wu, R.B. White, and M.N. Rosenbluth, Bull. Am. Phys. **39**, 1705 (1994).

12. H.L. Berk, B.N. Breizman, and M. Pekker, "Numerical Simulation of Bump-on-Tail Instability with Source and Sink," IFS Report No. 690, to be published in Phys. Plasmas **2**, 8 (1995).

13. B.N. Breizman, H.L. Berk, and H. Ye, Phys. Fluids B **5**, 3217 (1993).

14. H.L. Berk, B.N. Breizman, and H. Ye, Phys. Rev. Lett. **68**, 3563 (1992).

15. H.L. Berk, B.N. Breizman, J. Fitzpatrick, and H.V. Wong, "Line-Broadened Quasilinear Burst Model," to be published in Nuclear Fusion.

16. R.G. Littlejohn, J. Plasma Phys. **29** 111 (1983).

17. J.D. Meiss and R.D. Hazeltine, Phys. Fluids B **2**, 2563 (1990).

18. H.L. Berk, B.N. Breizman, and H. Ye, Phys. Lett. A **162**, 475 (1992).

19. B.N. Breizman and S.E. Sharapov, submitted to Plasma Phys. Contr. fus., Preprint IFSR 671, 1994.

FIGURE CAPTIONS

FIG. 1. Particle loading near the resonance.

FIG. 2. Resonant particle bounce frequency at mode saturation (initial value problem without a source and sink, and without background damping).

FIG. 3. Pulsating nonlinear regime for an isolated mode. The normalized background damping and the particle relaxation rate for this run are, respectively, $\gamma_d/\gamma_L = 0.15$ and $\frac{\nu_a}{\gamma_L} = 0.03$.

FIG. 4. Snapshot of the radial distribution function of resonant particles at the peak of the strongest burst shown in Fig. 3.

FIG. 5. Enhancement of the mode energy in the nonlinear pulsations of two overlapped modes with rspect to the single mode pulsations shown in Fig. 3.

FIG. 6. Benign pulsations of three modes without mode overlap: a) time evolution of the first mode energy; b) snapshot of the radial distribution of resonant particles. The normalized background damping and the particle relaxation rate for this run are, respectively, $\gamma_d/\gamma_L = 0.26$ and $\nu_a/\gamma_L = 0.039$.

FIG. 7. Particle loss simulation. Snapshots of the particle distribution function with $\gamma_d/\gamma_L = 0.22$ and $\nu_a/\gamma_L = 0.034$.

FIG. 8. Time evolution of the wave energy in the particle loss simulations shown in Fig. 7. Note the enhancement of the mode energy and synchronization of bursts caused by mode overlap.

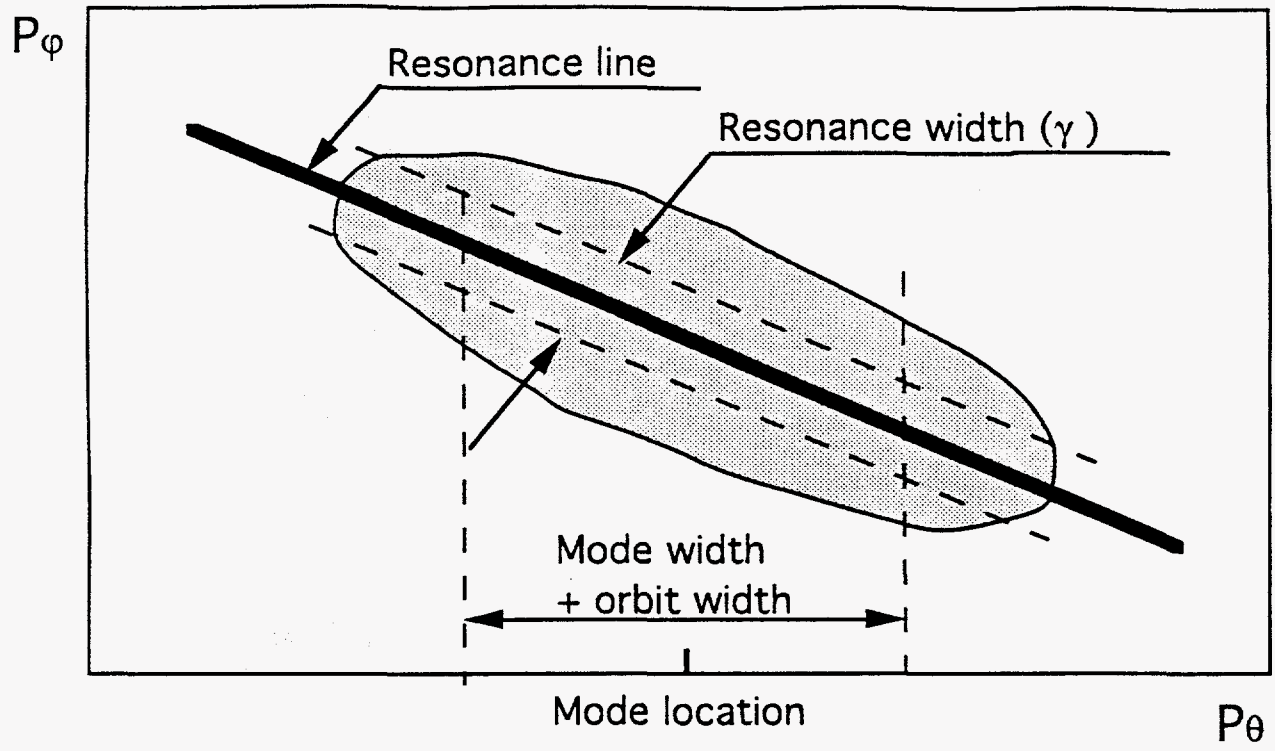

Figure 1

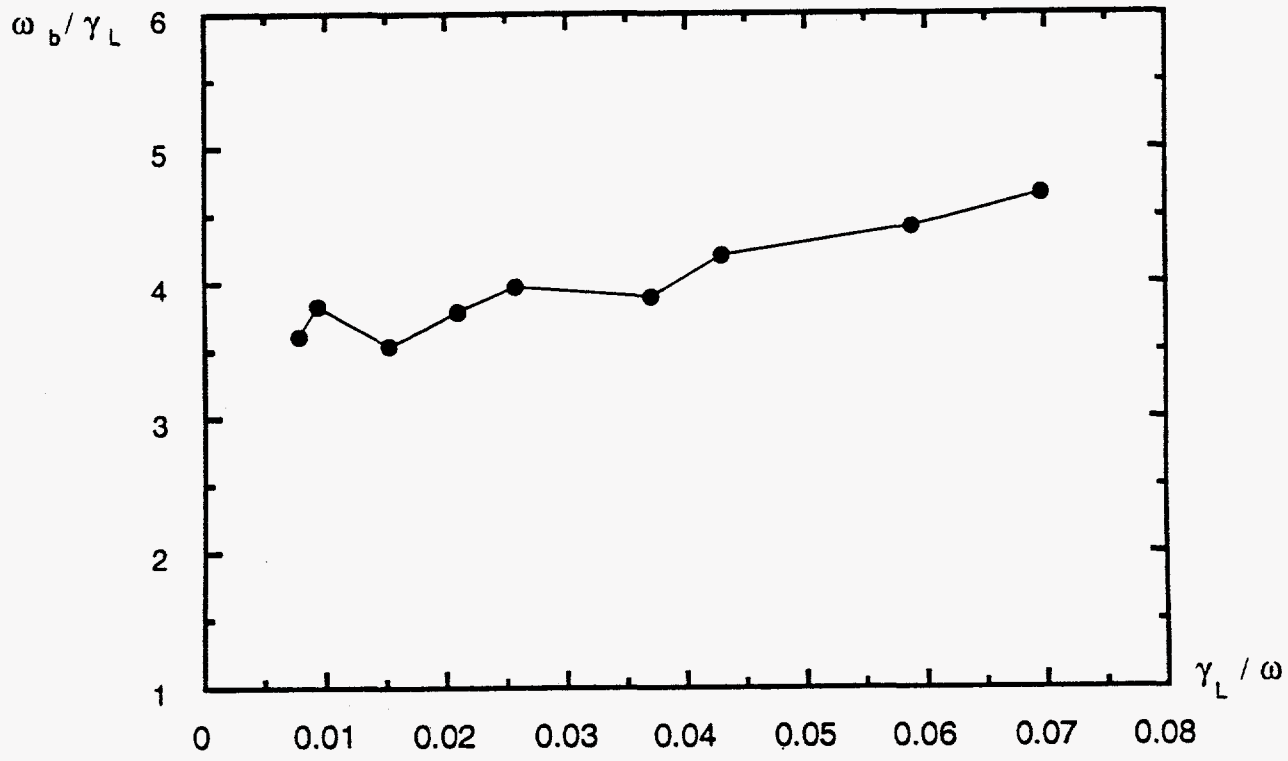

Figure 2

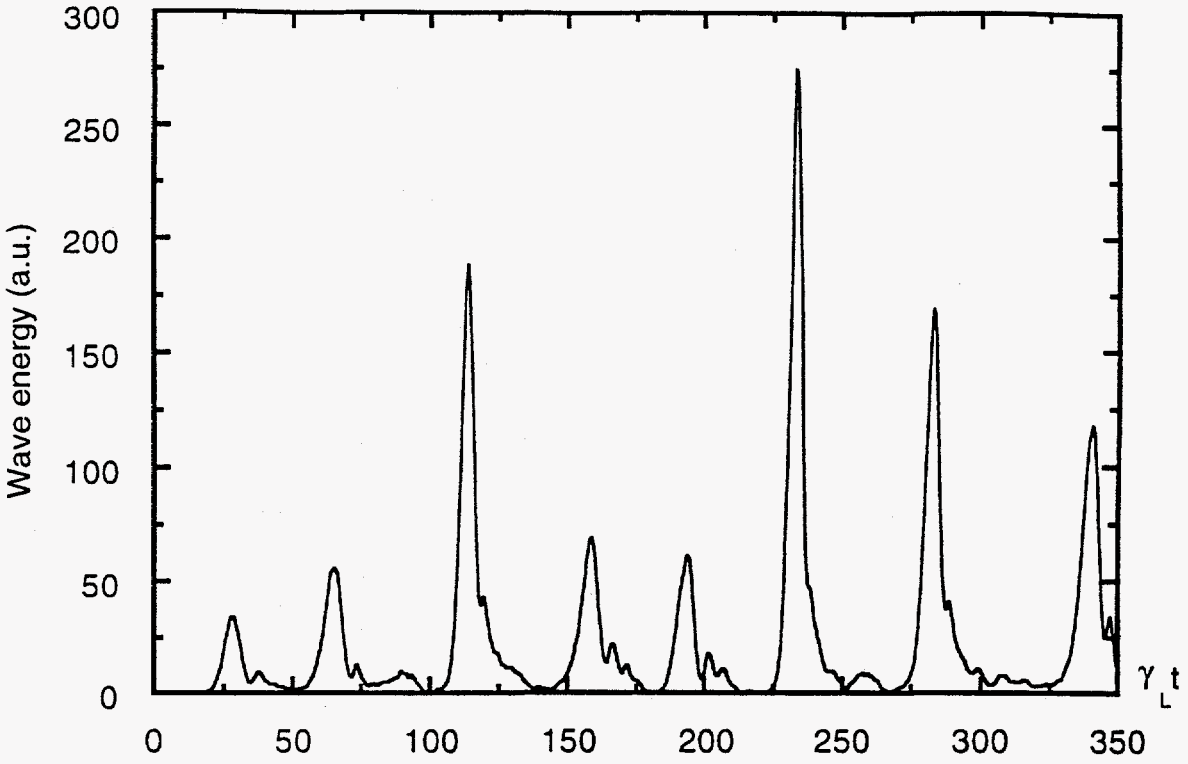

Figure 3

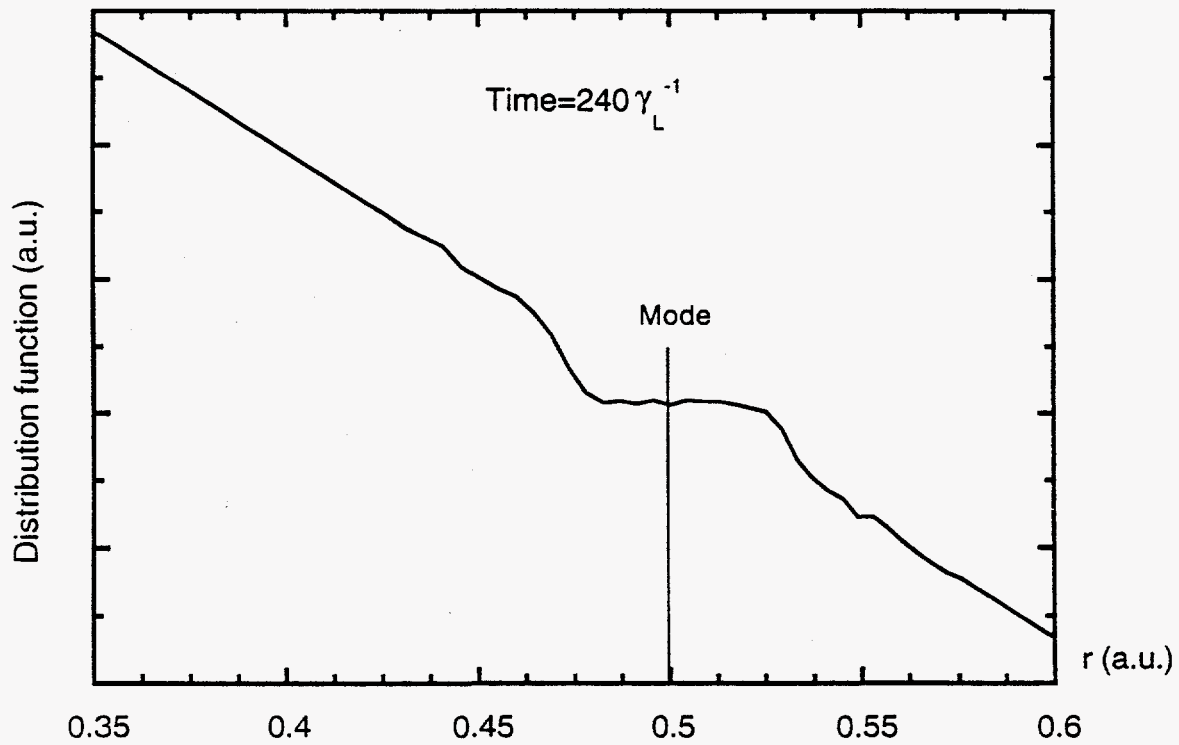

Figure 4

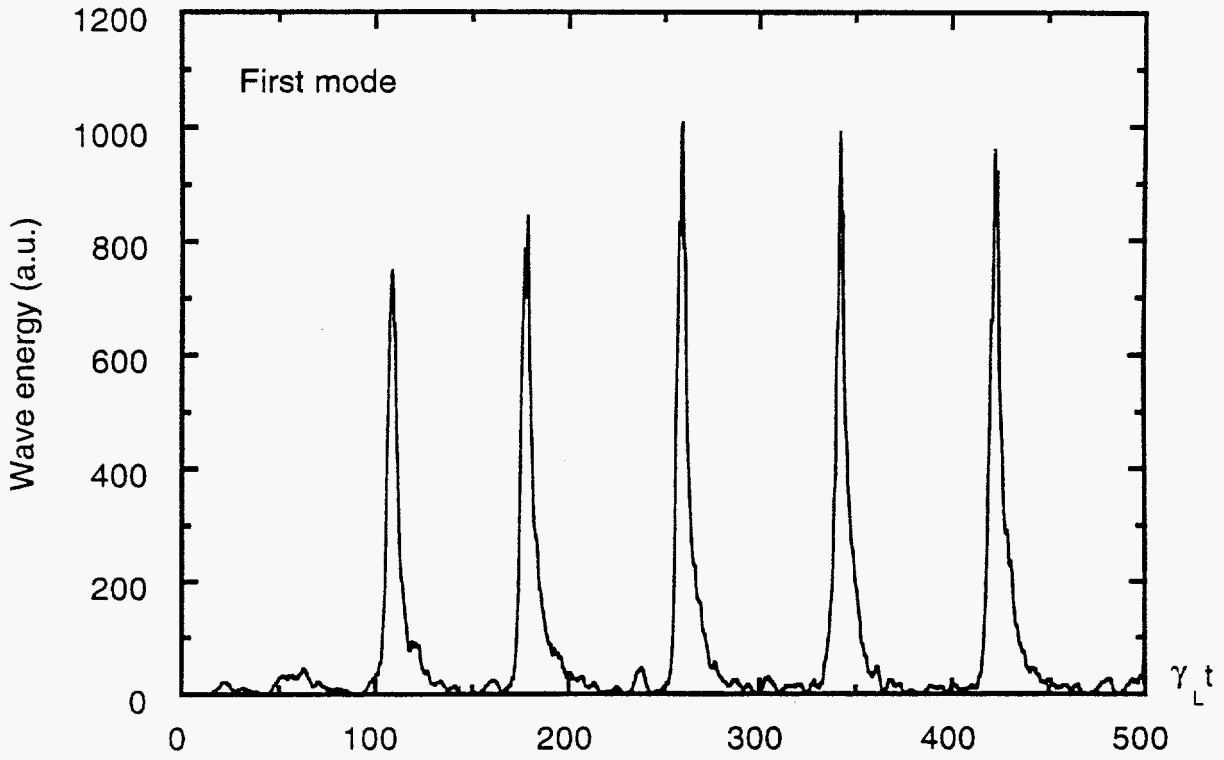
First mode
Wave energy (a.u.)
1200
1000
800
600
400
200
0
0
100
200
300
400
500
$\gamma_L t$

Figure 5

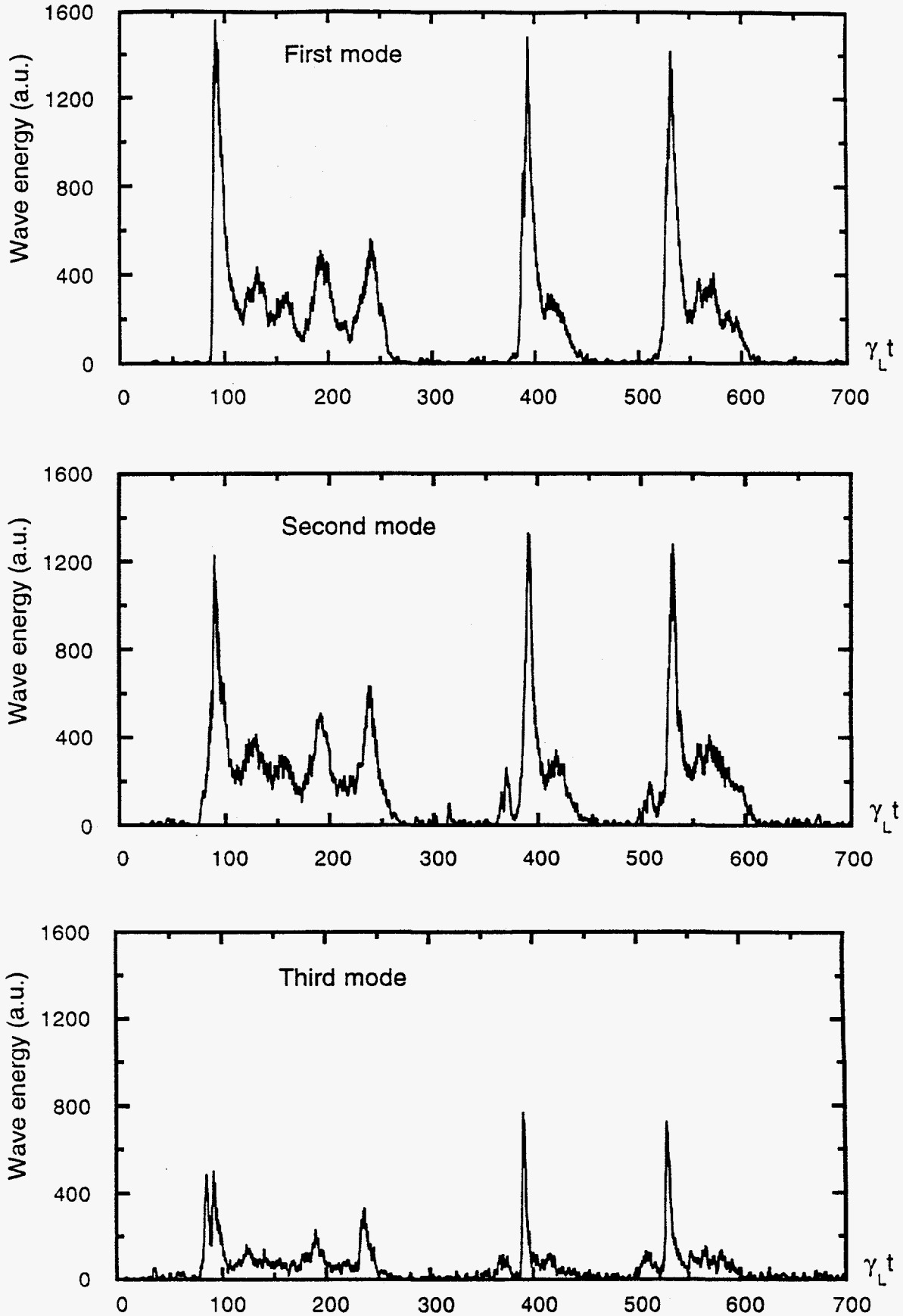
First mode
Second mode
Third mode
Wave energy (a.u.)
1600
1200
800
400
0
0
100
200
300
400
500
600
700
$\gamma_L t$

Figure 8